



Modification of Interfacial Tension and Wettability in Oil–Brine–Quartz System by in Situ Bacterial Biosurfactant Production at Reservoir Conditions: Implications for Microbial Enhanced Oil Recovery

Taehyung Park,[†] Min-Kyung Jeon,[†] Sukhwan Yoon,[†] Kun Sang Lee,[‡] and Tae-Hyuk Kwon^{*,†}

[†]Department of Civil and Environmental Engineering, Korea Advanced Institute of Science and Technology (KAIST), 291 Daehak-ro, Yuseong-gu, Daejeon, 34141, Korea

[‡]Department of Earth Resources and Environmental Engineering, Hanyang University, Seoul, 04763, Korea

S Supporting Information

ABSTRACT: Modification of oil–brine–minerals interfacial properties with biosurfactant-producing microorganisms and their extracellular metabolites has been considered as one of the viable strategies for microbial enhanced oil recovery (MEOR). In this study, the effect of lipopeptide biosurfactant produced by *Bacillus subtilis* on the interfacial tension (IFT) and wettability in oil–brine–mineral systems was quantitatively examined by monitoring dodecane–brine IFT and the contact angle of a dodecane–brine–quartz system during cultivation of *B. subtilis*. The effect of high temperature (35–45 °C) and pressure (~10 MPa), emulating conditions of in situ reservoir environments, on the effectiveness of the biosurfactant producers was also assessed using a custom-designed high-pressure bioreactor. Within the examined temperature range, it was confirmed that *B. subtilis* produced the lipopeptide biosurfactant (surfactin) with and without oxygen using nitrate (NO₃⁻) as the alternative electron acceptor. Thereby, the IFT was reduced from ~50 to ~10 mN/m and the wettability was modified from the values indicating an intermediate water-wet condition ($\theta = \sim 45\text{--}50^\circ$) to a strong water-wet condition ($\theta = \sim 20\text{--}25^\circ$). With the significantly improved capillary factor ($\gamma \cos \theta$) by a factor of 4.4, the two-phase flow simulations using the pore network model estimated significant increases in oil recovery rates in microbially treated reservoirs. The lowest rate and amount of surfactin production were observed at 45 °C, suggesting that higher temperatures may not be favorable for surfactin production by *Bacillus* spp. These results provide unique quantitative experimental evidence corroborating the feasibility of utilizing biosurfactant-producing microorganisms for MEOR practices targeting reservoirs with high pressure and moderately high temperature.

1. INTRODUCTION

Enhanced oil recovery (EOR) is a term encompassing various unconventional processes for enhancement of oil production from nearly depleted oil reservoirs.^{1,2} Commercial EOR strategies that are widely implemented in the oil industry include thermal injection, gas injection, and injection of synthetic chemicals, all of which are intended to alter capillarity in porous media.^{3–5} Applications of such techniques enable improved oil recovery from reservoirs, from which, otherwise, only 30–50% of crude oil are recoverable with conventional extraction during the primary recovery.⁶ The capillarity in porous media has a pronounced effect on the oil recovery rate and the displacement efficiency of water injection in a reservoir. Therefore, a better understanding of reservoir property improvements in oil–water interfacial tension (IFT) and oil–water–mineral wettability is thus critical for quantitative prediction of recovery efficiency, fluid injectivity, and oil recovery rate upon implementations of EOR techniques.

Use of synthetic chemical surfactants as additives to injection fluids has proved effective in EOR practices by reducing the capillary pressure of oil–brine–rock systems and hence increasing the oil production rates. Several biosurfactants, e.g., lipopeptides (i.e., surfactin and pumilacidin)⁷ and

glycolipids (i.e., rhamnolipids, sophorolipids, and trehalolipids)^{8–10} have been observed to have similar effects on the interfacial properties as the synthetic chemical surfactants. As biosurfactants are intrinsically innocuous and biodegradable, they have drawn attention as eco-friendly alternatives to chemical surfactants.^{11,12} Several microorganisms have been discovered to produce and excrete biosurfactants en masse, including strains affiliated to *Bacillus*, *Rhodococcus*, and *Pseudomonas* genera.¹³ Among these organisms, *Bacillus subtilis*, capable of producing lipopeptide biosurfactant (i.e., surfactin), have been regarded as suitable microorganisms for in situ biosurfactant production, due not only to their common presence in oil reservoirs, but also to their resilience to extreme environmental conditions, such as suboptimal pH and salinity, high pressure, and high temperature.^{14–19} The molecular structure of surfactin consists of a circular heptapeptide associated with a β -hydroxy fatty acid tail.^{15,17} Reportedly, surfactin, when applied as a concentrated additive, was capable of reducing the surface tension of water from 72 to ~28–30

Received: February 22, 2019

Revised: May 4, 2019

Published: May 13, 2019

mN/m, and the IFT between crude oil and water from 12.5 to ~0.5–5.8 mN/m.¹⁷

The repeated detection of the presence and activity of *Bacillus* spp. in oil reservoirs has motivated feasibility studies on the applicability of *B. subtilis* in microbial enhanced oil recovery (MEOR) in recent decades.^{15,17,20–22} One of the utmost challenges in such examinations was simulating in situ hydrocarbon reservoir conditions, which is often adverse to microbial inhabitation. Often, hydrocarbon reservoirs are found in deep subsurface, e.g., >1 km below the ground surface or seafloor surface. Thus, to emulate in situ reservoir conditions, laboratory experiments need to be conducted at high pressure (on the order of tens of megapascals) and at a range of temperatures that are substantially higher than the room temperature or optimal temperature range of *Bacillus* spp. (37 °C).²³ The paucity of literature reporting successful biologically mediated modification of interfacial properties at such high pressure and temperature conditions and quantitative experimental data hampers further development of a quantitative predictive model for capillary trapping in oil reservoirs. For the practical application of the biosurfactant producing bacteria in MEOR, a more thorough understanding of the *B. subtilis* metabolism and survivability at such hostile reservoir conditions is a prerequisite. In addition, evaluating the effectiveness of surfactin exuded by *Bacillus* spp. at the simulated in situ condition in modifying the interfacial property is crucial, given the oft-insufficient quantities of biosurfactants produced in vivo.

Therefore, the potential of biosurfactant-producing bacteria as a biocatalytic agent of MEOR was assessed by quantitatively examining microbial growth and metabolism and by monitoring the associated alterations in interfacial properties. A series of experiments was conducted, where the model organism *B. subtilis* strain ATCC6633 was cultured under fluid pressures of ~10 MPa and varying the temperature from 35 to 45 °C. At the same time, alterations in oil–brine IFT and oil wettability on quartz was evaluated, in which the quartz substrate was chosen to represent silicate rock minerals as the major component of sandstones.^{24–26} The impact of biosurfactant-induced modification of interfacial properties on oil displacement efficiency in a porous medium was further evaluated by conducting pore-scale two-phase flow simulation using the pore network model (PNM).

2. MATERIALS AND METHODS

2.1. Model Bacteria for Biosurfactant Production. In this study, *B. subtilis* strain ATCC6633 was selected as the model organism. Due mainly to the omnipresence of *Bacillus* spp. in subsurface and aquatic environments and their survivability under harsh environments such as extreme pH, high salinity,¹⁶ high temperature, and high pressure,²⁷ *Bacillus* spp. have been investigated as the model organisms for MEOR or geologic carbon storage (GCS) practices.^{15,17,18,28,29} Furthermore, their ability to form endospores supports their high survivability when subjected to extreme temperature, desiccation, and chemical disinfectants.¹⁹ Additionally, *Bacillus* spp. have been reported to be found in oil reservoirs, which includes ones in the United States (Oklahoma¹⁶), in Brazil (Atlantic Ocean, offshore Rio de Janeiro¹⁴), and in Japan (Minami-aga Oil field³⁰); this supports the selection of *Bacillus* strain as the model microorganism to evaluate MEOR.

2.2. Culture Conditions and Inoculum Preparation. *B. subtilis* strain ATCC6633 (KCTC2189) was acquired from the Korean Collection for Type Culture, and a mineral salt medium was used as a culture medium, following previous studies, as listed in Table 1.¹⁸ The mineral salt medium contained adequate amounts of carbon

Table 1. Composition of Mineral Salt Medium Used for Surfactin Production

compound	concentration
carbon source	
glucose	40 g/L
nitrogen source	
NH ₄ Cl	0.1 M
NaNO ₃	0.118 M
mineral salt medium	
MgSO ₄	8.0 × 10 ⁻⁴ M
CaCl ₂	8.0 × 10 ⁻⁴ M
FeSO ₄	8.0 × 10 ⁻⁴ M
Na ₂ EDTA	8.0 × 10 ⁻⁴ M
MnSO ₄	8.0 × 10 ⁻⁴ M
phosphate buffer	
KH ₂ PO ₄	0.03 M
Na ₂ HPO ₄	0.04 M

(glucose), nitrogen (nitrate and ammonium), and trace elements (manganese, potassium, iron, etc.), as suggested in previous experimental studies on surfactin production optimization (Table 1^{31–35}). This mineral salt medium was filter-sterilized prior to use (0.2 μm sterile syringe filter; Chmlab Group, Terrassa-Barcelona, Barcelona, Spain).

The inoculum for the experiments was prepared by inoculating 1 mL of frozen stock culture to 100 mL of fresh nutrient broth (Difco, BD, Franklin Lakes, NJ, USA). After 24 h of incubation at 37 °C without shaking, 4 mL of this fresh culture was transferred to filter-sterilized mineral salt medium for the IFT and wettability experiments.

2.3. Mineral Substrate and Surface Modification. In this study, a square-shaped quartz disk (25 × 25 × 5 mm; Sungho Sigma, Gyeonggi-do, South Korea) was used as a solid substrate for the investigation of wetting phenomena. This quartz disk was selected for its smooth and flat surface as a rough surface may cause hysteresis in contact angle measurement.

In spite of the innate hydrophilicity of quartz minerals, the rock minerals of sandstone oil reservoirs are found to range from weakly water-wet, to neutral-wet, to weakly oil-wet, often with the contact angle larger than 30–60°.^{36,37} Therefore, the quartz substrate was aged in dodecane, in which the quartz disk was autoclaved at 121 °C and soaked in filter-sterilized dodecane for more than 30 days at 50 °C. Upon this aging process, the contact angle of dodecane–brine on the aged quartz substrate was approximately 50°, which represents a weakly water-wet condition.

2.4. Experimental Setup. The experimental setup was designed to measure and monitor the changes in IFT and contact angle during microorganism cultivation under high pressure and various temperature conditions emulating actual oil reservoir conditions. As shown in Figure S1, a stainless steel high pressure vessel with an internal volume of 40 cm³ was constructed, and it was equipped with two quartz crystal windows to monitor the wettability changes in real time (i.e., view cell). IFT was measured by using the pendant drop method (Figure 1A), and the contact angle was measured by using the sessile drop method (Figure 1B). To measure the dodecane–brine IFT, the inner volume of the cell was first filled with brine to culture microorganisms, and the capillary tube with an outer diameter of 1.59 mm produced oil droplets. The contact angle of the oil–brine–quartz system was measured by placing an oil droplet on the quartz disk using the capillary tube (i.e., Figure 1B).

For this study, a high-pressure syringe pump (500HP, Teledyne Isco, Lincoln, NE, USA) was used to pressurize the view cell and the transfer vessels, as shown in Figure 1 and Figure S1. One transfer vessel contained dodecane and the other contained brine, respectively; thereby, the high-pressure syringe pump fed pressurized deionized water (DIW) to the transfer vessels to inject dodecane or oil into the view cell at a controlled flow rate under elevated pressure

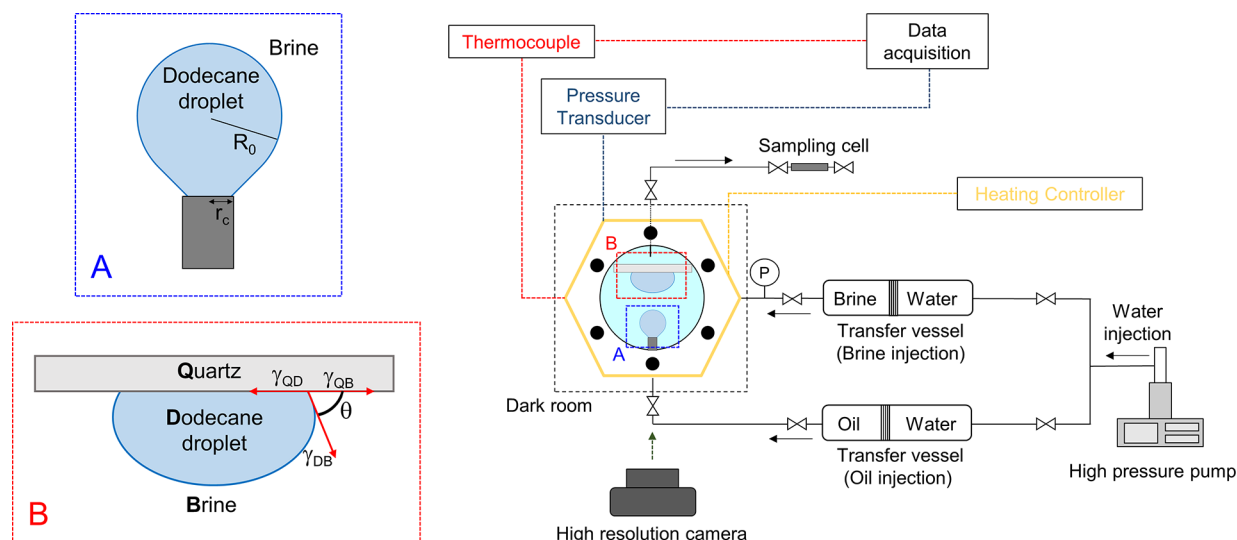


Figure 1. Schematic of the experimental system for interfacial tension (IFT) (A) and contact angle (B) measurement.

(Figure S1). A high-resolution digital single-lens-reflex (DSLR) camera (Canon EOS 100D, Canon 100 mm 2.8f macro lens) was used to acquire droplet imageries. A coil-type electric heater was installed to control the temperature inside the view cell, and the temperature was monitored with a K-type thermocouple (Hankook Electric Heater, South Korea). A pressure transducer (PX302, Omega, Norwalk, CT, USA) was also installed to monitor fluid pressure inside the view cell. The temperature and pressure were logged with a data logger with a 10-s interval (34970A, Keysight, Santa Rosa, CA, USA).

2.5. Experimental Procedures. In this study, experiments at three different temperatures (35, 40, and 45 °C) were run under a pressure of 10 MPa. All wetting parts, including tubes, fittings, valves, and transfer vessels, were autoclaved at 120 °C, and the inner space of the view cell was sterilized with 70% ethyl alcohol for more than 12 h. For cultivation of *B. subtilis* in the view cell, 4 mL of the culture grown in the broth medium was inoculated inside the view cell that was filled with 40 mL of the fresh mineral salt medium. Thereafter, one transfer vessel contained 100 mL of the fresh mineral salt medium, and the view cell was pressurized to 10 MPa by injecting the fresh medium from the transfer vessel. During the pressurization process, air in the headspace was completely displaced with the medium through a fluid port located at the top. When the pressure and temperature inside the view cell were stabilized at the target values, oil droplets were generated through the capillary tube for IFT and contact angle measurements.

For the IFT measurement of oil–brine, a pendant droplet of dodecane was maintained under stable temperature–pressure conditions. Over the course of microbial growth and the biosurfactant production, time-lapsed images of dodecane on the capillary tube were acquired every minute for ~60 h. The images were analyzed with the low bond axisymmetric drop shape analysis (LBDSA) method that fitted a first-order approximation of the Young–Laplace equation using a plugin for ImageJ software.³⁸ For high accuracy of the pendant drop method, the bond number defined as the dimensionless ratio of a buoyance force-to-surface force ratio was controlled to be in the range of 0.1–0.9 by adjusting the volume of oil drops.³⁹

For the contact angle measurement, a dodecane droplet was carefully positioned on the quartz disk which was aged for more than 30 days, as shown in Figure 1B. Upon the positioning of a dodecane sessile droplet on the quartz substrate, the time-lapsed images were acquired every minute for ~60 h during microbial growth and biosurfactant production. The contact angles of dodecane–brine–quartz in the acquired images were determined using the drop-snake plugin for ImageJ software.⁴⁰ Although Young’s angle is theoretically irrelevant to the size of droplet, the volume of the dodecane droplet was kept to be less than 10 μL for reliable and consistent estimates. In general, 5–10 μL drops are regarded the appropriate droplet size for

contact angle measurement.⁴¹ Additionally, the difference between the contact angles of the right and left edges was controlled to be less than 2%, and thereby these right- and left-side contact angle values were averaged to determine consistent contact angle values. The images for oil droplets in brine for IFT and contact angle measurements before and after surfactin production are shown in Figure S2.

A total of six runs were carried out: three temperatures for IFT measurement and three temperatures for contact angle measurement, respectively. In all test runs, approximately 1 mL of samples was acquired every 4–5 h to quantify the concentrations of surfactin, glucose, nitrate, and ammonium in the brine phase (or growth medium). Upon sampling, the high-pressure syringe pump pressurized the view cell back to 10 MPa, compensating for the pressure loss due to sampling volume. Changes in the metabolite concentrations (i.e., surfactin, glucose, nitrate, and ammonium) in the view cell by the sampling volume were unavoidable but considered to be insignificant.

2.6. Product Analysis. The fluid samples acquired during the experiments were analyzed for the concentrations of biosurfactant, carbon source (glucose), and nitrogen sources (nitrate and ammonium). Upon sampling, the acquired fluid samples were immediately filter-sterilized to remove cell mass and insoluble biomass, preventing further microbial growth. These filter-sterilized samples were then stored at –20 °C until analysis.

The concentration of surfactin was determined using a high-performance liquid chromatography (HPLC) system (Shimadzu LC-20AD Prominence) equipped with a reverse phase C18 column (Shimadzu Shim-pack GIS, 250 \times 4.6 mm; Shimadzu, Kyoto, Japan) with the oven temperature set to 40 °C. The detection absorbance was set to 205 nm, and the mobile phase was 3.8 mM trifluoroacetic acid/acetonitrile (1:4, v/v) with a flow rate of 1 mL/min. Per sample, 20 μL was injected for this biosurfactant analysis. The calibration curves were constructed with surfactin standard (Sigma-Aldrich, St. Louis, MO, USA). The glucose concentration in the samples as carbon source was also quantified using the standard glucose oxidase assay kit (Sigma-Aldrich, St. Louis, MO, USA). The concentrations of ammonium and nitrate as nitrogen sources in the samples were analyzed with a Humas kit (HS-NH3(N)-L, HS-NO3(N)-CA; Humas, South Korea).

2.7. Pore Network Modeling Simulation. To examine the effectiveness of biosurfactant on enhanced oil recovery, the pore network model (PNM) was developed and used for two-phase flow simulation. A PNM is a network built by idealizing the geometry and interconnectivity of pores in a porous medium; it consists of spherical pore bodies and cylindrical throats. Quasi-static multiphase flow simulations in such a PNM appeared to be the best representatives to

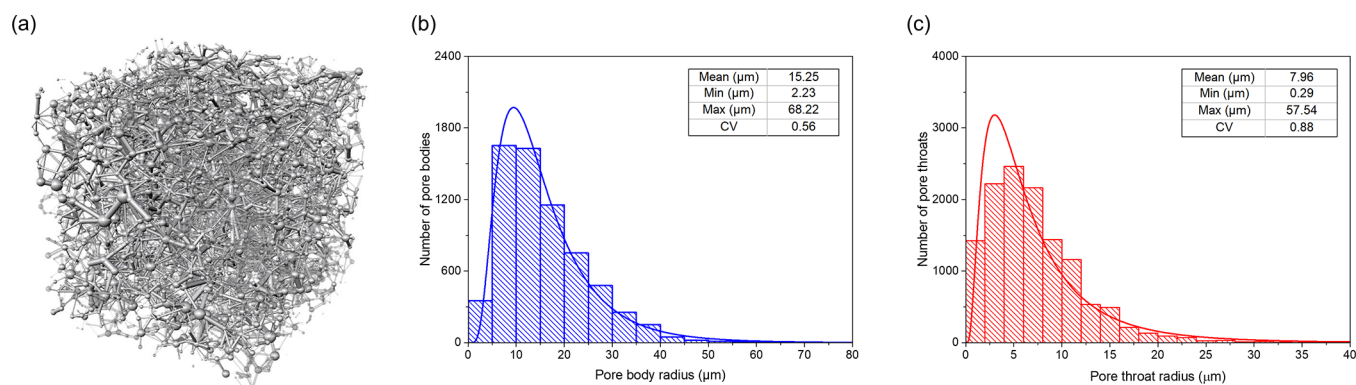


Figure 2. Extracted pore network of Berea sandstone micro-CT images (a),⁴⁴ and distributions of pore radii (b) and pore throat radii (c) of the Berea sandstone pore network used in PNM simulation.

simulate the core experiments.⁴² Accordingly, quasi-static water flooding was simulated to a dodecane-saturated Berea sandstone which is widely used as a natural porous rock. First, the PNM of this Berea sandstone was extracted and constructed by using its micro computed tomography (micro-CT) image set that is publicly shared;⁴³ the image set has $400 \times 400 \times 400$ pixels with $5.345 \mu\text{m}$ resolution. Based on the maximal ball algorithm,⁴⁴ the PNM of Berea sandstone was constructed with 6518 pores and 12 508 throats, as shown in Figure 2.

Second, the quasi-static two-phase flow simulation was performed in this extracted PNM, following the method suggested by Valvatne and Blunt.⁴² Herein, the entire network was saturated with oil (dodecane), and water was then injected, displacing dodecane in the network. Thus, water was set as the invading fluid, and dodecane was set as the displaced fluid. The two-phase flows in the PNM were simulated at various differential pressure conditions from 10 kPa to 1 MPa, and hence the residual oil saturations at corresponding capillary pressures were obtained. The details of this PNM flow simulation can be found in previous studies.^{18,42,44,45} Table 2 shows the input

Table 2. Input Parameters for PNM Simulations

	case 1	case 2
experimental conditions		
surfactant	no	yes
temperature ($^{\circ}\text{C}$)	35	35
pressure (MPa)	10	10
time (h)	0	60.2
experimental results		
IFT (mN/m)	50	8
contact angle (deg)	49	24
capillary factor ($\gamma \cos \theta$) (mN/m)	33	7.5
input parameters for PNM simulation		
viscosity of water (mPa·s)		0.72
viscosity of CO_2 (mPa·s)		1.29
mean radius of pore (μm)		15.25
mean radius of pore throats (μm)		7.96
COV of pore radius		0.56
COV of pore throat radius		0.88

parameters for two-phase PNM simulations, where the IFT of dodecane–brine and contact angle of dodecane–brine–quartz with and without biosurfactant were acquired from experimental results from this study.

3. RESULTS

3.1. Microbial Cultivation and Surfactin Production.

During the cultivation of biosurfactant producing bacteria, *B. subtilis*, in a defined medium at 35, 40, 45 $^{\circ}\text{C}$ and 10 MPa, the

concentrations of surfactin and carbon and nitrogen sources were monitored. Figures 3 and 4 present the production of surfactin and the consumptions of glucose, nitrate, and ammonium during the cultivation of *B. subtilis* at the reservoir conditions in a medium containing 40 g/L glucose, 10 g/L nitrate, and 5 g/L ammonium. With the fluid samples acquired every 4 h, the growth of *B. subtilis* and the production of surfactin were confirmed with gradual changes in the product concentrations, as consumption of glucose, nitrate, and ammonium provided direct evidence of microbial metabolism. In particular, glucose, nitrate, and ammonium were not completely depleted in all tests (Figures 3 and 4), which indicated that, in these tests, carbon and nitrogen sources were hardly limited during the cultivation.

The trends of glucose concentration followed the typical trends of bacterial cell growth for 10–20 h and then gradually decreased over the course of cultivation periods. The glucose was similarly depleted in all conditions examined: the concentration reached a plateau after ~ 30 h of rapid decrease. In the IFT and contact angle experiments at 35, 40, and 45 $^{\circ}\text{C}$, 34.1, 37.3, and 29.1 g/L and 31.3, 33.6, and 30.6 g/L glucose were consumed, respectively. As the optimal temperature for the growth of *B. subtilis* is reported to be ~ 37 $^{\circ}\text{C}$,^{23,46} the glucose consumptions at 45 $^{\circ}\text{C}$ was the least compared to those at 35 and 40 $^{\circ}\text{C}$. It can be explained by the lowered microbial activity at the high temperature. This is consistent with the temperature effect on surfactin production, which is shown in section 4.2.

It is worth paying attention to the sequential reductions in ammonium first and then nitrate. First, rapid reductions in ammonium concentration were observed immediately upon onset of *B. subtilis* incubation (Figures 3 and 4). The ammonium concentration decreased from 5 to ~ 3 g/L for the first 12 h, and thereafter stayed constant at a value of ~ 3 g/L. To be specific, during the IFT experiments, 2.0, 2.5, and 2.1 g/L ammonium were consumed, where 2.1, 3.0, and 2.4 g/L ammonium were consumed during the contact angle experiments at 35, 40, and 45 $^{\circ}\text{C}$, respectively. During this interval where the ammonium was actively being consumed, i.e., the first 12 h, no significant reduction of nitrate concentration was observed. After 12 h when the ammonium consumption rate was significantly diminished, a clear decline in nitrate concentration was observed. During the IFT experiments, 6.2, 3.0, and 4.0 g/L nitrate were consumed at 35, 40, and 45 $^{\circ}\text{C}$. In the contact angle experiments 3.0, 4.9, and 3.6 g/L nitrate were consumed at 35, 40, and 45 $^{\circ}\text{C}$, respectively.

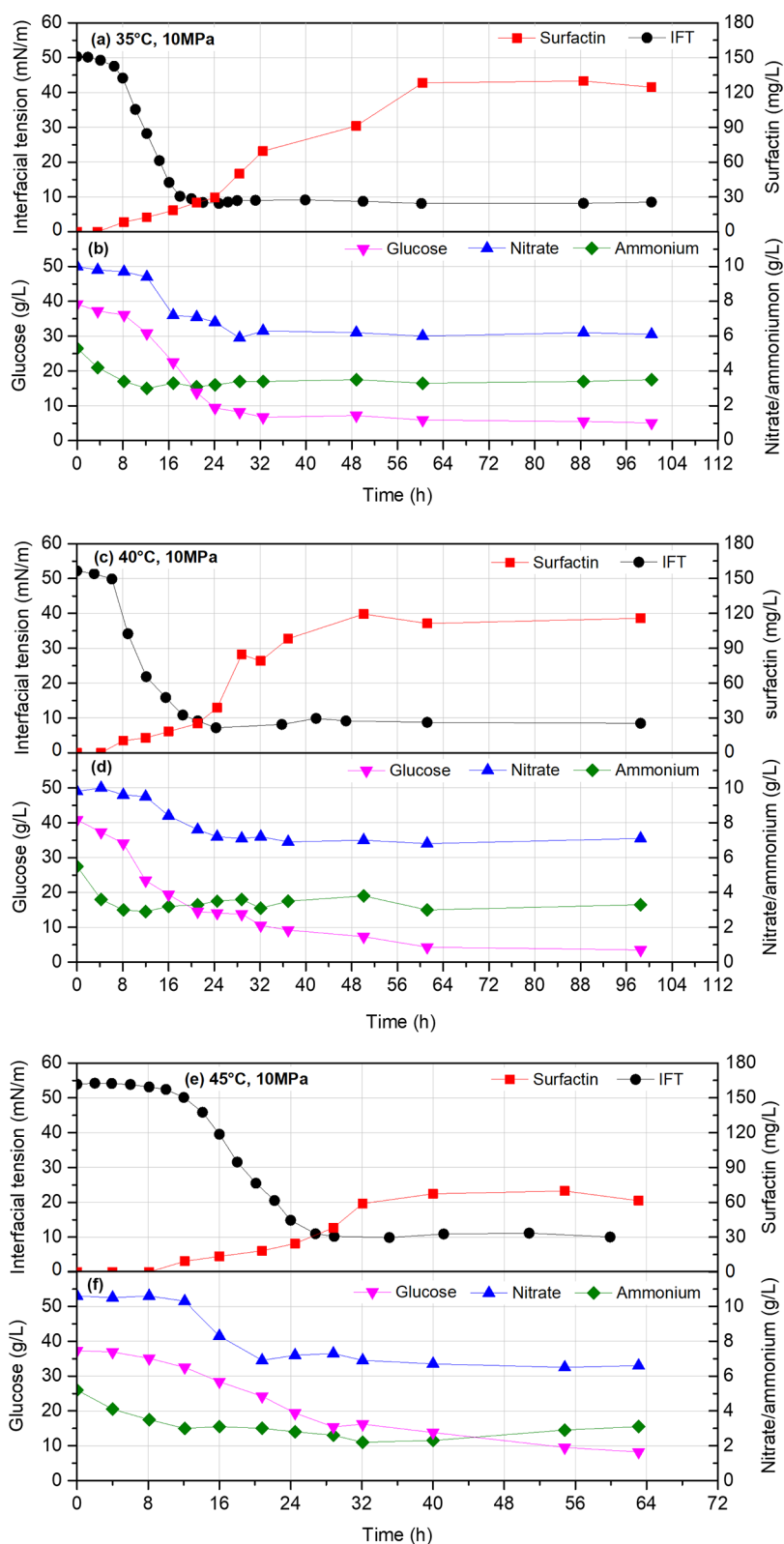


Figure 3. Variations in dodecane/brine IFT and surfactin concentration (35 (a), 40 (c), and 45 °C (e)) and glucose, nitrate, and ammonium (35 (b), 40 (d), and 45 °C (f)) during the cultivation of *B. subtilis* at various temperatures and 10 MPa.

Furthermore, it was observed that the concentration of surfactin gradually increased with the cultivation of *B. subtilis*. At both 35 and 40 °C, the surfactin concentration became detectable after 8 h. On the contrary, at 45 °C, the surfactin was detected after 12 h, which indicates the delayed

production of surfactin at a temperature higher than 45 °C. The final concentration of surfactin at 35 and 40 °C ranged 106–125 mg/L, and the surfactin production at 35 °C was slightly more than that at 40 °C. Whereas the final concentration of surfactin at 45 °C was 61–73 mg/L, the

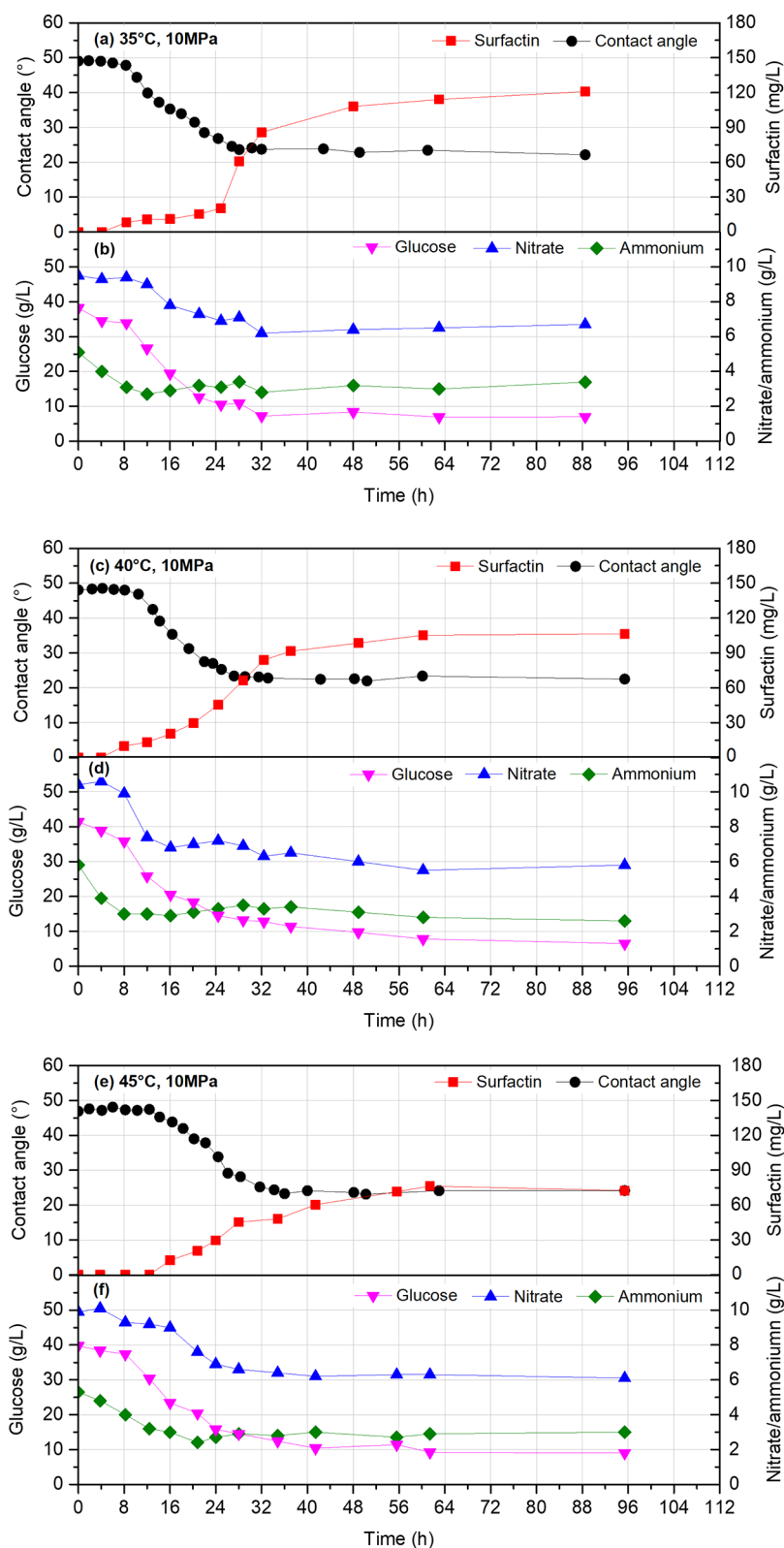


Figure 4. Variations in contact angle of dodecane–brine–quartz and surfactin concentration (35 (a), 40 (c), and 45 °C (e)) and glucose, nitrate, and ammonium (35 (b), 40 (d), and 45 °C (f)) during the cultivation of *B. subtilis* at various temperatures and 10 MPa.

lowest amount of surfactin was produced, presumably owing to the high temperature.

3.2. Variation in Dodecane–Brine IFT by in Situ Biosurfactant Production. Parts a, c, and e of Figure 3 show the variations in the dodecane–brine IFT during the growth of

B. subtilis at 35, 40, and 45 °C, respectively. The IFT value was determined from the pendant droplet curvature of dodecane surrounded by the growth medium (Figure 1A).

In all the examined temperature conditions, clear reductions in IFT were observed with the surfactin production by *B.*

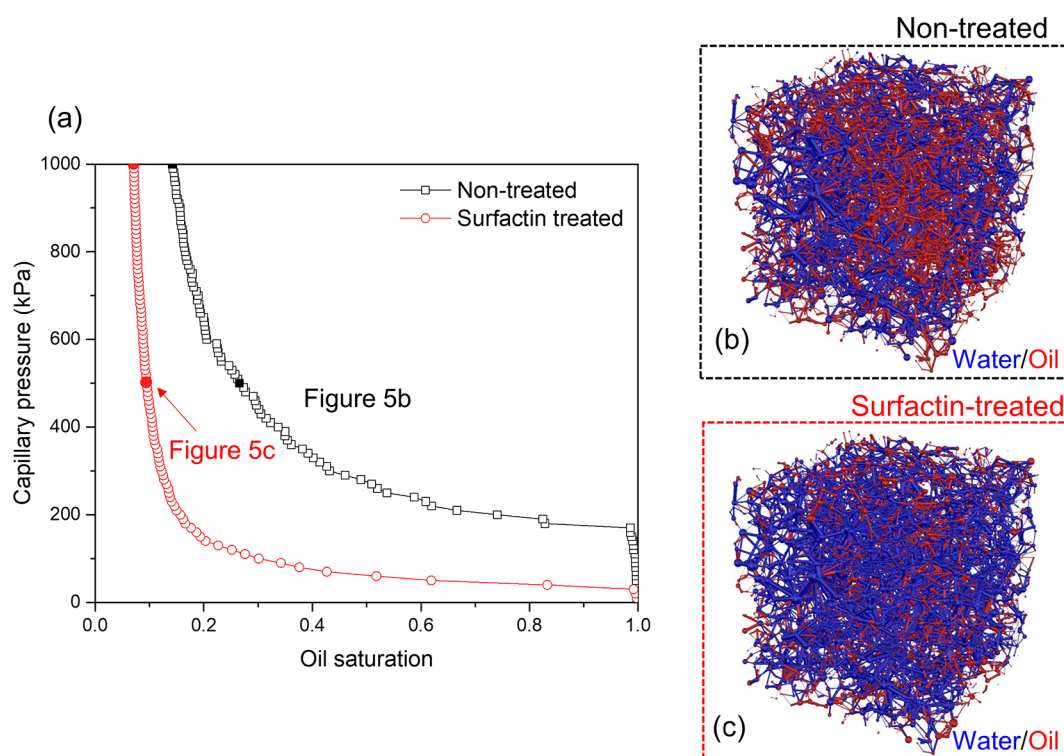


Figure 5. (a) PNM simulation results of residual oil saturation with and without surfactin treatments. Images of the pore network upon water flooding at the pressure of 500 kPa into dodecane-filled pore network without surfactin treatment (b) and with surfactin treatment (c).

subtilis. With the initial rapid production surfactin, the IFT of dodecane and brine decreased from ~ 50 – 54 to ~ 8 – 10 mN/m, showing the reduction by 42–44 mN/m. This occurred within the time frame of less than 30 h. Thereafter, the IFT values converged to and stayed at the lower limit, approximately 8–10 mN/m. It is presumed that 30–40 mg/L surfactin is sufficient to reduce the IFT to the lower limit, taking into consideration the interfacial area of the pendant droplet used for IFT measurement (Figure 3). Considering the surfactin production was significantly less at 45 °C, it is worth noting that the initial and final IFT values were fairly consistent regardless of temperatures. This implies that the surfactin was sufficiently produced even at 45 °C to reduce the IFT, exceeding the critical concentration.

Despite the narrow range of the examined temperature range, the delayed onset of IFT reduction and the slowed rate of IFT reduction by the elevated temperature were found, particularly for 45 °C. The onset of IFT reduction matched closely with the detection of surfactin production. Accordingly, the onset of IFT reduction was ~ 6.5 and ~ 6.1 h after the inoculation at 35 and 40 °C, respectively. Meanwhile, the onset of IFT reduction at 45 °C was at ~ 10.5 h, delayed by ~ 4 h compared to those at 35 and 40 °C. Upon such onsets of IFT reduction, the rate of IFT reduction was estimated to be 2.0, 2.0, and 1.5 mN/(m·h) for 35, 40, and 45 °C, respectively. Not only the growth kinetics, but also the rate of IFT reduction, was the slowest at 45 °C, compared with those at 35 and 40 °C.

3.3. Variation in Dodecane–Brine–Quartz Contact Angle by in Situ Biosurfactant Production. Parts a, c, and e of Figure 4 show the variations in dodecane–brine–quartz contact angle during the growth of *B. subtilis* at 35, 40, and 45 °C, respectively. The contact angle was monitored from the sessile droplet generated from the capillary tube being placed

on a quartz plate (Figure 1B). In all cases, reductions in contact angle were observed with the increasing concentration of surfactin. Owing to the surfactin production during *B. subtilis* growth, the contact angle decreased from ~ 48 – 49 to $\sim 23^\circ$, showing the reduction by 25–26°. The gradual reduction of contact angle was observed within 30 h, and then converged to and stayed at the lower limit, approximately 23°. Taking into consideration the surface area of the sessile droplets, 40–60 mg/L surfactin was sufficient to reduce the contact angle to the lower limit (Figure 4). Similar to the observation from the 45 °C IFT experiment, the initial and final contact angle values were fairly constant regardless of temperature, whereas the surfactin production was remarkably less at the 45 °C contact angle experiment. It is presumed that a sufficient amount of surfactin was produced even at 45 °C to modify wettability.

The delayed onset of contact angle reduction was observed at elevated temperature. At 35 and 40 °C, the onset of contact angle modification was ~ 8 h after the inoculation, whereas that of the 45 °C experiment was 12 h, delayed by ~ 4 h compared to 35 and 40 °C cases. The rate of contact angle reduction was estimated to be 0.9, 0.9, and 0.6 deg/h for 35, 40, and 45 °C, respectively. Both the growth kinetics and the rate of contact angle reduction were the slowest at 45 °C, which corresponds to the observations during IFT experiments.

3.4. PNM Results on Displacement Efficiency in Oil Recovery Rate with Biosurfactant. The two-phase flow simulations were conducted using PNM (hereafter PNM simulation) to evaluate the improvement of oil recovery by biosurfactant-producing bacteria, *B. subtilis*. Figure 5 shows the residual oil saturation against the capillary pressure for the given input values of IFT and contact angle of the dodecane–brine–quartz system. Herein, the capillary pressure is the pressure difference between the inlet and outlet pores, and the

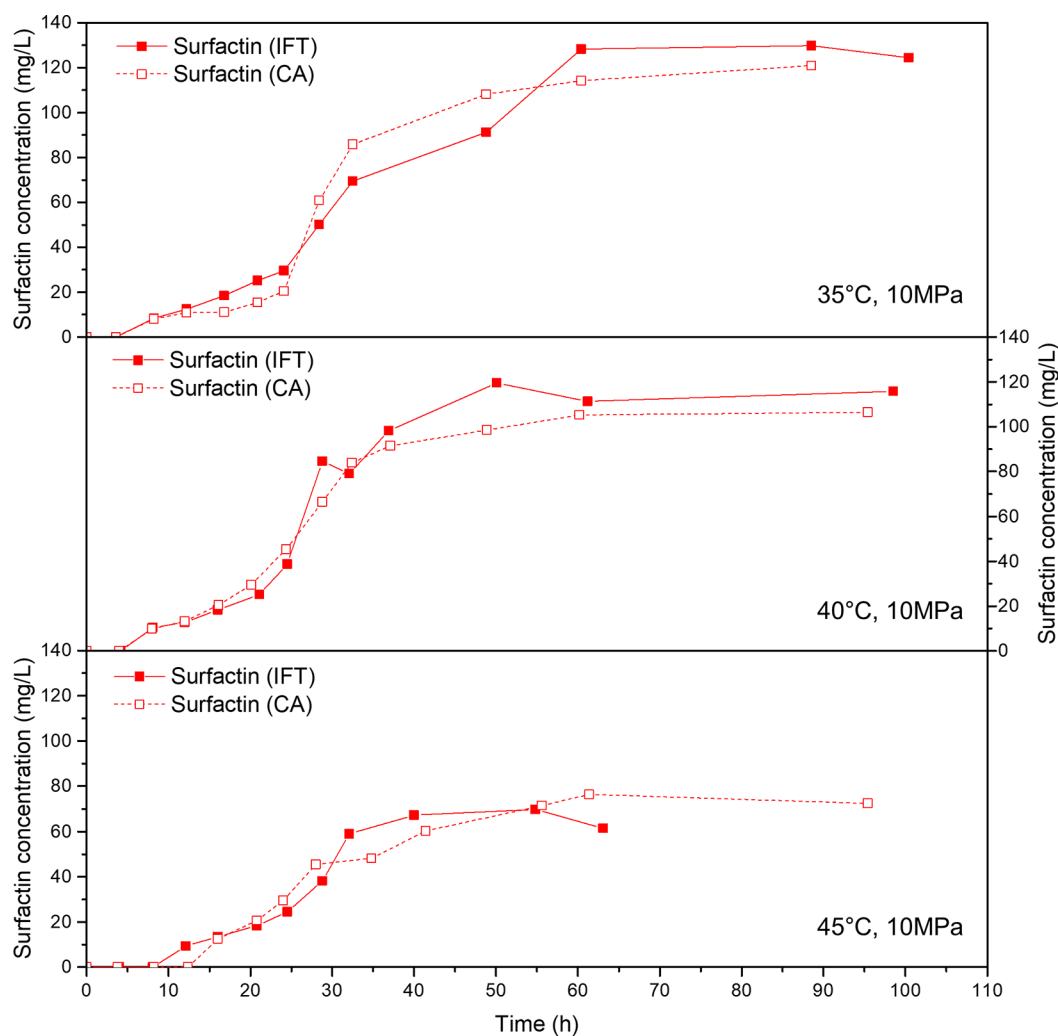


Figure 6. Surfactin production rates under different temperature conditions. Both the surfactin concentrations determined in the IFT and contact angle experiments are plotted.

residual oil saturation is defined as the ratio of the pore volume occupied by oil to the entire pore volume of the network after displacement.

Figure 5a highlights that, for a given capillary pressure (or pressure difference), the residual oil saturation was lowered with the altered interfacial properties by surfactin. Such lowered residual oil saturation implies that more oil can be displaced or swept by water flooding, mainly due to the lowered capillary factor (i.e., defined as $\gamma \cos \theta$). For instance, when water was injected at 500 kPa, as the capillary factor decreased from 33 to 7.5 mN/m, the residual oil saturation was 0.27 without surfactin, but it decreased to 0.09 when the interfacial properties of water–oil–rock surface were modified by the biosurfactant. Parts b and c of Figure 5 show the invasion patterns of water into the dodecane-saturated pore network with and without surfactin treatment, respectively. It can be clearly seen that the surfactin-treated pore network (Figure 5c) is more filled with water than the nontreated network. Again, this confirms that the lowered IFT and wettability alteration by biosurfactant leads to the reduction in residual oil saturation, and hence to the improved displacement efficiency and the enhanced oil recovery rate. The PNM results of reduced capillary factor lead to the improved displacement efficiency in porous media consistent with the

previous studies that the sweep efficiency of CO_2 improved as the surfactants modified the interfacial properties of CO_2 .^{18,45}

4. ANALYSIS AND DISCUSSION

4.1. Utilization of Nitrate for Surfactin Production in Anoxic Conditions. The biosurfactant-producing bacterium *B. subtilis* appears to produce surfactin readily under a high fluid (water) pressure condition of 10 MPa, which is equivalent to a water depth of ~ 1 km. In the view cell, the high-water pressure was maintained at 10 MPa with no headspace, which indicates microoxic conditions with minimally available free oxygen during the microbial cultivation and surfactin production. Interestingly, it was noted in all tests that the ammonium was preferably utilized over the nitrate (Figures 3 and 4). This indicated that *B. subtilis* utilized the ammonium when the dissolved oxygen was available in brine. Once the dissolved oxygen was deleted, *B. subtilis* began to consume nitrate as a terminal electron acceptor in the absence of oxygen. The results corroborate previous findings that several types of Gram-positive bacteria, such as *B. subtilis* and *Streptomyces venezuelae*, preferentially consume ammonium over nitrate in the presence of oxygen.^{47,48} Furthermore, the results showed that the onset of nitrate consumption coincided with the sudden acceleration of surfactin production rate.

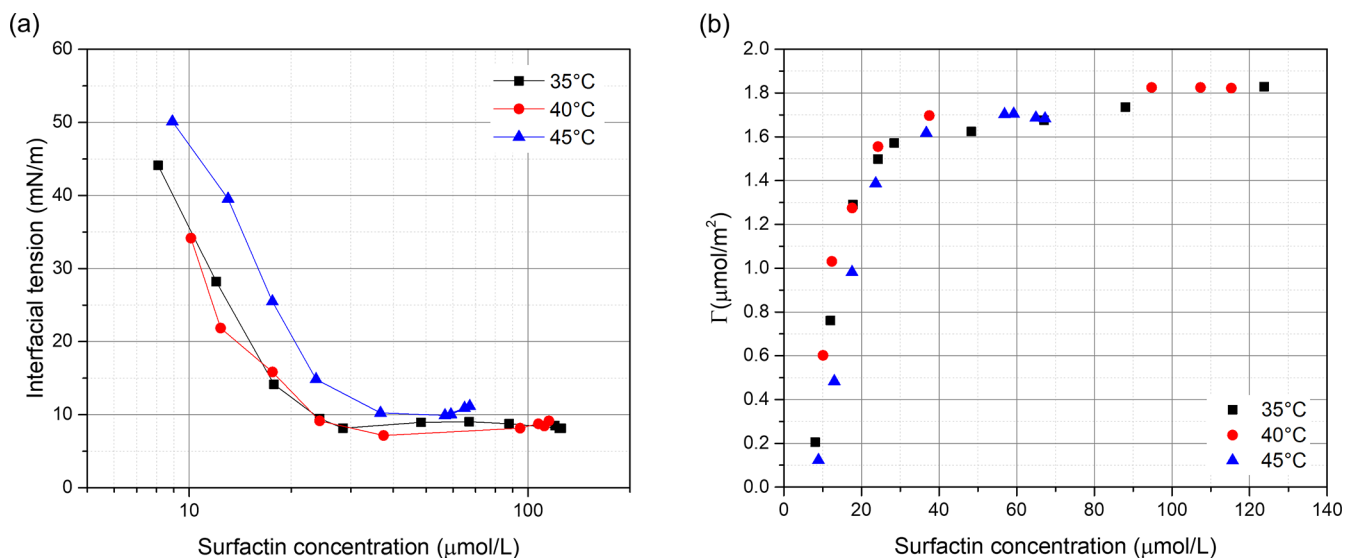


Figure 7. (a) Changes of IFT as a function of surfactin concentration and (b) variations in surface excess concentration against surfactin concentration.

Davis et al. have also observed the rapid increment in surfactin production as the dissolved oxygen depleted in the growth medium, and the following nitrate utilizing metabolisms was initiate.⁴⁷

The results have an important implication that microbial production of surfactin is feasible in both aerobic and anaerobic conditions, as long as a proper terminal electron acceptor, nitrate for example, exists in the environment. Further, adequate injection strategy can be applied to instantly stimulate surfactin production with the controls of nitrogen sources depending on the oxygen availability.

4.2. Effect of Temperature on Surfactin Production by *B. subtilis*. *B. subtilis* was capable of producing surfactin in the temperature range 35–45 °C, as shown in Figures 3 and 4. Because the final concentrations of surfactin exceeded the critical micelle concentration (cmc) in all tested temperatures, alterations in IFT and contact angle were consistently to the possible maximum extent in such temperatures (e.g., from ~50–54 to ~8–10 mN/m for IFT; from ~48–49 to ~23° for contact angle) with the reduction in capillary factor by ~75–77%. However, when comparing the final surfactin concentrations with respect to the temperature (Figure 6), the microbial growth and surfactin production were relatively restricted at 45 °C. *B. subtilis* produced ~110–130 mg/L surfactin at 35 and 40 °C; whereas ~70–80 mg/L surfactin was produced at 45 °C. This indicates that the microbial activities of *B. subtilis* including surfactin production differ with temperature and can be limited further at temperature greater than 45 °C.

The finding also implies the significance of temperature as one of the governing factors dominating the biosurfactant production rate and oil recovery to determine the success or failure of MEOR. In situ temperature of hydrocarbon reservoirs typically ranges from ambient temperature for shallow reservoirs, such as oil sand deposits, to a temperature hotter than 100 °C for deep reservoirs at the depth of 2–3 km, such as shale gas reservoirs. From the perspectives of petroleum geology, reservoirs can be called *hot* reservoirs (>100 °C), *medium-temperature* reservoirs (50 < T < 100 °C), and *cold* reservoirs (<50 °C). The temperature of the targeted

sedimentary formations is presumed to determine the success of application of *Bacillus* spp. for MEOR as it has a profound effect on biosurfactant production. *Bacillus* spp. are expected to be applicable for MEOR practices in “cold” reservoirs with temperatures less than 50 °C. Meanwhile, this still warrants further investigation to examine the surfactin production rate at temperatures higher than 45 °C.

4.3. Adsorption Characteristics of Surfactin at Oil–Brine Interfaces. The adsorption characteristics of surfactin at reservoir conditions are important information to evaluate the potential of using surfactin for MEOR practices. The adsorption characteristics include the critical micelle concentration (cmc), surface excess concentration, and minimum surface area occupied per surfactant molecule at monolayer adsorption. Most previous studies have examined the surfactin adsorbed at air–water interfaces, which may not be applicable to the condition at oil–brine interfaces with various co-ions/counterions.⁴⁹ Therefore, the surfactin adsorption characteristics at oil–brine interfaces under elevated pressure and temperature close to reservoir conditions are examined herein.

The difference in IFT values with a biosurfactant at its critical micelle concentration (γ_{cmc}) and without the biosurfactant (γ_0) represents the effectiveness of the biosurfactant; the effectiveness of the lipopeptide biosurfactant, surfactin, produced by *B. subtilis* at 35, 40, and 45 °C and 10 MPa can be described as follows:

$$\pi_{cmc} = \gamma_0 - \gamma_{cmc} \quad (1)$$

Additionally, the surface excess concentration (Γ_{max} ; in $\mu\text{mol}/\text{m}^2$) of the surfactin can determined by the reduction in dodecane–brine IFT with respect to the change in surfactin concentration according to the Gibbs equation, as follows:⁵⁰

$$\Gamma_{max} = -\frac{1}{2.303nRT} \lim_{c \rightarrow cmc} \left(\frac{d\gamma}{d \log S} \right) \quad (2)$$

where γ is the dodecane–brine IFT (in mN/m), R is the gas constant (8.314 J/mol K), T is the absolute temperature (K), S is the surfactin concentration (mol/L), and n is the number of species at the dodecane–brine interface, which is assumed to be 1 in this study. With the computed surface excess

concentration value, the minimum surface area (A_{\min}) occupied per surfactin molecule at monolayer adsorption is calculated by the following equation:

$$A_{\min} = \frac{10^{18}}{N_A \Gamma_{\max}} \quad (3)$$

where N_A is Avogadro's number (6.022×10^{23}).

Figure 7a shows the changes in dodecane–brine IFT with the surfactin concentration for 35, 40, and 45 °C. Accordingly, the critical micelle concentration (cmc), the effectiveness (π_{cmc}), the surface excess concentration (Γ_{max}), and the minimum surface area per surfactin molecule (A_{\min}) are computed based on the experiment results, as listed in Table 3.

Table 3. Interfacial Properties of Surfactin Produced from This Study

temp (°C)	cmc ($\mu\text{mol/L}$)	π_{cmc} (mN/m)	Γ_{max} ($\mu\text{mol/m}^2$)	A_{\min} (\AA^2)
35	28.4	42.2	1.57	106
40	37.5	45.0	1.69	97.9
45	36.7	43.7	1.62	103

The critical micelle concentration (cmc) ranges 28–38 $\mu\text{mol/L}$ at 35, 40, and 45 °C and 10 MPa, as shown in Figure 7a, and the effectiveness (π_{cmc}) is 42–45 mN/m. From the slopes of $\gamma/\log S$ in Figure 7a, the surface excess concentration (Γ_{max}) is computed to be 1.6–1.7 $\mu\text{mol/m}^2$, and hence the minimum surface area per surfactin molecule (A_{\min}) is 98–106 \AA^2 . These values of the cmc, effectiveness, surface excess concentration, and minimum surface area per surfactin are found to be fairly consistent within the tested temperature range.

Figure 7b shows the variations in surface excess concentration with the surfactin concentration. It appears that the surface excess concentration approaches asymptotic close to ~ 1.6 – $1.7 \mu\text{mol/m}^2$, equivalent to $\sim 100 \text{\AA}^2$, as the surfactin concentration exceeds $\sim 40 \mu\text{M}$, regardless of temperature. In previous studies,^{49,51} the surface excess concentration and the minimum surface area of surfactin dissolved in pure deionized water have been reported to range 1.02–1.05 $\mu\text{mol/m}^2$ and 159–170 \AA^2 for air–water interfaces in ambient conditions, respectively. The values obtained in this study (Γ_{max} , A_{\min}) appear consistent with those from the previous studies,^{49,51} while the differences in fluids (oil versus air), ionic concentration, and temperature possibly caused the observed differences in these values. This result shows that the surfactin maintains its functionality as a surface-active agent at oil–brine interfaces in such extreme and complex environments, and thus proposes that surfactin produced by *Bacillus* spp. can be used as a biochemical agent to enhance hydrocarbon recovery in MEOR practices.

4.4. Implication for Microbial Enhanced Oil Recovery (MEOR). The main strategy of MEOR practices may vary as to whether the microbes to be are either indigenous (biostimulation) or exogenous (bioaugmentation).⁵² Recently, the biostimulation strategy using indigenous bacteria was proposed to minimize ecological disturbance and to avoid competition over nutrients among exogenous and indigenous microorganisms, overcoming the limitations of ex situ bioaugmentation strategy such as the low efficiency and the difficulties in monitoring microbial activities of bioaugmented bacteria during MEOR.^{53–57} Meanwhile, *Bacillus* species, the same species as the model bacterium used in this study, is one of the most widely found microorganisms in deep oil reser-

voirs.^{14–17,20,22,27,30,54,58,59} Therefore, when metagenomics analysis of the produced fluid samples from a candidate oil reservoir reveals the presence of indigenous and active *Bacillus* spp., injection of nutrients to stimulate those species can be an effective way to enhance oil recovery.

On the contrary, only minimal amounts and minimal activities of microorganisms are often detected in some hydrocarbon reservoirs, possibly attributed to their high temperature. For such microbially nonactive reservoirs, the bioaugmentation strategy using exogenous microbes can be readily applied. However, caution should be exercised that the inoculated microbes must adapt to the reservoir conditions, such as temperature, pressure, salinity, and pH, as the microbial growth is greatly affected by those factors.^{60,61} *B. subtilis* is tolerant against high fluid pressures, salinity, and a wide range of pH; *B. subtilis* is thus expected to be generally applicable for “cold” reservoirs with a temperature less than 50 °C, as confirmed in this study. Besides, *B. subtilis* is known to be capable of production of biofilms⁶² and biogenic gases,⁶³ which aids enhanced oil recovery (EOR) via selective plugging and/or providing pressure support, respectively. Nevertheless, detailed examination as to what extent in situ reservoir temperature and high salinity conditions (especially in the presence of divalent cations) retards surfactin production of *B. subtilis* should be carried out prior to field implementation.

In addition, other numerous environmental factors, such as salinity, pH, rock mineralogy, oil type, and, most importantly, type of indigenous microorganisms, can also influence the extent of bacterial alteration of IFT and wettability during the MEOR process. With previous studies, this study corroborates evidence to the applicability of stimulating *Bacillus* spp. under reservoir conditions for MEOR; nevertheless, implementation of in situ bacterial biosurfactant production for MEOR, using either bioaugmentation or biostimulation, would require site-specific investigation because of the diversity of hydrocarbon reservoir conditions.

5. CONCLUSION

This study investigated the potential of biosurfactant-producing bacteria, *Bacillus subtilis* as an enhancer of MEOR at high pressure and various temperature conditions. The extent of dodecane–brine IFT reduction and oil wettability alteration during the cultivation of *B. subtilis* at reservoir conditions was experimentally conducted at different temperature conditions. The dodecane–brine IFT decreased and the contact angles of dodecane–brine–quartz increased with the growth of *B. subtilis* and following surfactin production and soon reached the lower and upper limits as the system reached critical micelle concentration (cmc). The presented experimental results clearly show that *B. subtilis*, the biosurfactant-producing bacteria, can be an excellent mediator to treat rock mineral surfaces to be more water-wet in complex oil–brine–mineral systems and to reduce oil–brine IFT even at high pressure and warm temperature (35–45 °C) in both aerobic and anaerobic conditions. The experiments revealed similar trends, but comparing the 35 and 40 °C cases with the 45 °C case, the growth and surfactin production kinetics were slower at 45 °C, where the surfactin production was also the lowest at the highest temperature conditions. Further, the pore network model (PNM) results support that the reduced capillary factor from ~ 33 to ~ 7.5 mN/m can enhance oil recovery rate by decreasing the residual oil saturation from 27 to 9% and increasing the displacement rate.

Given the frequent appearance of *Bacillus* spp. from oil reservoir, this study provides comprehension of a biostimulation technique for MEOR. Not only the biostimulation technique but also the bioaugmentation technique is expected to be a prospective technique for MEOR, as this study confirmed the feasibility of *B. subtilis* as an enhancer of MEOR at reservoir conditions, such as at high pressure, high salinity, and various temperature conditions.

■ ASSOCIATED CONTENT

📄 Supporting Information

The Supporting Information is available free of charge on the ACS Publications website at DOI: 10.1021/acs.energyfuels.9b00545.

Photograph of experimental systems for interfacial tension and contact angle measurements during microbial cultivation at high-pressure, high-temperature conditions; images of oil droplets for IFT and contact angle measurements before and after microbial growth and surfactin production (PDF)

■ AUTHOR INFORMATION

Corresponding Author

*Tel.: +82-42-350-3628. Fax: +82-42-869-3610. E-mail: t.kwon@kaist.ac.kr.

ORCID

Sukhwan Yoon: 0000-0002-9933-7054

Tae-Hyuk Kwon: 0000-0002-1610-8281

Notes

The authors declare no competing financial interest.

■ ACKNOWLEDGMENTS

This research was supported by a grant (19CTAP-C151917-01) from the Technology Advancement Research Program (TARP) funded by the Ministry of Land, Infrastructure and Transport of the Korean government, and by a National Research Foundation of Korea (NRF) grant funded by the Korean government (Ministry of Science, ICT & Future Planning) (No. 2017R1C1B2007173).

■ REFERENCES

- (1) Lake, L. W. *Enhanced Oil Recovery*; Prentice Hall: 1989.
- (2) Lake, L. W.; Johns, R. T.; Rossen, W. R.; Pope, G. A. *Fundamentals of Enhanced Oil Recovery*; Society of Petroleum Engineers: 2014.
- (3) Sheng, J. J. Enhanced oil recovery in shale reservoirs by gas injection. *J. Nat. Gas Sci. Eng.* **2015**, *22*, 252–259.
- (4) Butler, R. M. *Thermal Recovery of Oil and Bitumen*; Prentice Hall: 1991.
- (5) Baviere, M.; Glenat, P.; Plazenet, V.; Labrid, J. Improvement of the efficiency/cost ratio of chemical EOR processes by using surfactants, polymers, and alkalis in combination. *SPE Reservoir Eng.* **1995**, *10* (3), 187–193.
- (6) Lundquist, A.; Cheney, D.; Powell, C.; O'Neill, P.; Norton, G.; Veneman, A.; Evans, N.; Mineta, S.; Abraham, S.; Allbaugh, J. Energy for a new century: increasing domestic energy production. *Reliable, Affordable, and Environmentally Sound Energy for America's Future: Report of the National Energy Policy Development Group*; U.S. Government Printing Office: 2001; pp 70–90.
- (7) Jacques, P. Surfactin and Other Lipopeptides from *Bacillus* spp. In *Biosurfactants*; Springer: 2011; pp 57–91.
- (8) Daverey, A.; Pakshirajan, K. Sophorolipids from *Candida bombicola* using mixed hydrophilic substrates: production, purification and characterization. *Colloids Surf., B* **2010**, *79* (1), 246–253.
- (9) Benincasa, M.; Abalos, A.; Oliveira, I.; Manresa, A. Chemical structure, surface properties and biological activities of the biosurfactant produced by *Pseudomonas aeruginosa* LBI from soap-stock. *Antonie van Leeuwenhoek* **2004**, *85* (1), 1–8.
- (10) White, D.; Hird, L.; Ali, S. Production and characterization of a trehalolipid biosurfactant produced by the novel marine bacterium *Rhodococcus* sp., strain PML026. *J. Appl. Microbiol.* **2013**, *115* (3), 744–755.
- (11) Desai, J. D.; Banat, I. M. Microbial production of surfactants and their commercial potential. *Microbiol. Mol. Biol. Rev.* **1997**, *61* (1), 47–64.
- (12) Ron, E. Z.; Rosenberg, E. Natural roles of biosurfactants. *Environ. Microbiol.* **2001**, *3* (4), 229–236.
- (13) Soberón-Chávez, G.; Maier, R. M. Biosurfactants: A General Overview. In *Biosurfactants*; Springer: 2011; pp 1–11.
- (14) Da Cunha, C. D.; Rosado, A. S.; Sebastián, G. V.; Seldin, L.; Von der Weid, I. Oil biodegradation by *Bacillus* strains isolated from the rock of an oil reservoir located in a deep-water production basin in Brazil. *Appl. Microbiol. Biotechnol.* **2006**, *73* (4), 949–959.
- (15) Al-Bahry, S.; Al-Wahaibi, Y.; Elshafie, A.; Al-Bemani, A.; Joshi, S.; Al-Makhmari, H.; Al-Sulaimani, H. Biosurfactant production by *Bacillus subtilis* B20 using date molasses and its possible application in enhanced oil recovery. *Int. Biodeterior. Biodegrad.* **2013**, *81*, 141–146.
- (16) Simpson, D. R.; Natraj, N. R.; McInerney, M. J.; Duncan, K. E. Biosurfactant-producing *Bacillus* are present in produced brines from Oklahoma oil reservoirs with a wide range of salinities. *Appl. Microbiol. Biotechnol.* **2011**, *91* (4), 1083.
- (17) Al-Wahaibi, Y.; Joshi, S.; Al-Bahry, S.; Elshafie, A.; Al-Bemani, A.; Shibulal, B. Biosurfactant production by *Bacillus subtilis* B30 and its application in enhancing oil recovery. *Colloids Surf., B* **2014**, *114*, 324–333.
- (18) Park, T.; Joo, H.-W.; Kim, G.-Y.; Kim, S.; Yoon, S.; Kwon, T.-H. Biosurfactant as an Enhancer of Geologic Carbon Storage: Microbial Modification of Interfacial Tension and Contact Angle in Carbon dioxide/Water/Quartz Systems. *Front. Microbiol.* **2017**, *8*, 1285.
- (19) Nicholson, W. L.; Munakata, N.; Horneck, G.; Melosh, H. J.; Setlow, P. Resistance of *Bacillus* endospores to extreme terrestrial and extraterrestrial environments. *Microbiol. Mol. Biol.* **2000**, *64* (3), 548–572.
- (20) Liu, Q.; Lin, J.; Wang, W.; Huang, H.; Li, S. Production of surfactin isoforms by *Bacillus subtilis* BS-37 and its applicability to enhanced oil recovery under laboratory conditions. *Biochem. Eng. J.* **2015**, *93*, 31–37.
- (21) Pereira, J. F.; Gudiña, E. J.; Costa, R.; Vitorino, R.; Teixeira, J. A.; Coutinho, J. A.; Rodrigues, L. R. Optimization and characterization of biosurfactant production by *Bacillus subtilis* isolates towards microbial enhanced oil recovery applications. *Fuel* **2013**, *111*, 259–268.
- (22) Pornsunthorntawe, O.; Arttaweeporn, N.; Paisanjit, S.; Somboonthanate, P.; Abe, M.; Rujiravanit, R.; Chavadej, S. Isolation and comparison of biosurfactants produced by *Bacillus subtilis* PT2 and *Pseudomonas aeruginosa* SP4 for microbial surfactant-enhanced oil recovery. *Biochem. Eng. J.* **2008**, *42* (2), 172–179.
- (23) Ohno, A.; Ano, T.; Shoda, M. Production of a lipopeptide antibiotic, surfactin, by recombinant *Bacillus subtilis* in solid state fermentation. *Biotechnol. Bioeng.* **1995**, *47* (2), 209–214.
- (24) Morrow, N. R. Wettability and Its Effect on Oil Recovery. *JPT, J. Pet. Technol.* **1990**, *42* (12), 1476–1484.
- (25) Lamb, R. N.; Furlong, D. N. Controlled wettability of quartz surfaces. *J. Chem. Soc., Faraday Trans. 1* **1982**, *78* (1), 61–73.
- (26) Bera, A.; Ojha, K.; Kumar, T.; Mandal, A.; S, K. Mechanistic study of wettability alteration of quartz surface induced by nonionic surfactants and interaction between crude oil and quartz in the presence of sodium chloride salt. *Energy Fuels* **2012**, *26* (6), 3634–3643.

- (27) Yakimov, M. M.; Timmis, K. N.; Wray, V.; Fredrickson, H. L. Characterization of a new lipopeptide surfactant produced by thermotolerant and halotolerant subsurface *Bacillus licheniformis* BASS0. *Appl. Environ. Microbiol.* **1995**, *61* (5), 1706–1713.
- (28) Peet, K. C.; Freedman, A. J.; Hernandez, H. H.; Britto, V.; Boreham, C.; Ajo-Franklin, J. B.; Thompson, J. R. Microbial growth under supercritical CO₂. *Appl. Environ. Microbiol.* **2015**, *81* (8), 2881–2892.
- (29) Kwon, T.-H.; Park Geological storage system of carbon dioxide and process for geological storage of carbon dioxide. U.S. Patent Appl. 16,052,781, 2019.
- (30) Kato, T.; Haruki, M.; Imanaka, T.; Morikawa, M.; Kanaya, S. Isolation and characterization of long-chain-alkane degrading *Bacillus thermoleovorans* from deep subterranean petroleum reservoirs. *J. Biosci. Bioeng.* **2001**, *91* (1), 64–70.
- (31) Cooper, D. G.; Goldenberg, B. G. Surface-active agents from two *Bacillus* species. *Appl. Environ. Microbiol.* **1987**, *53* (2), 224–229.
- (32) Shaligram, N. S.; Singhal, R. S. Surfactin—a review on biosynthesis, fermentation, purification and applications. *Food Technol. Biotechnol.* **2010**, *48* (2), 119–134.
- (33) Wei, Y.-H.; Chu, I.-M. Mn²⁺ improves surfactin production by *Bacillus subtilis*. *Biotechnol. Lett.* **2002**, *24* (6), 479–482.
- (34) Wei, Y.-H.; Lai, C.-C.; Chang, J.-S. Using Taguchi experimental design methods to optimize trace element composition for enhanced surfactin production by *Bacillus subtilis* ATCC 21332. *Process Biochem.* **2007**, *42* (1), 40–45.
- (35) Rangarajan, V.; Clarke, K. G. Towards bacterial lipopeptide products for specific applications—a review of appropriate downstream processing schemes. *Process Biochem.* **2016**, *51* (12), 2176–2185.
- (36) Dullien, F. A. *Porous Media: Fluid Transport and Pore Structure*; Academic Press: 2012.
- (37) Øren, P.-E.; Bakke, S. Reconstruction of Berea sandstone and pore-scale modelling of wettability effects. *J. Pet. Sci. Eng.* **2003**, *39* (3–4), 177–199.
- (38) Daerr, A.; Mogne, A. Pendent_drop: an imagej plugin to measure the surface tension from an image of a pendent drop. *J. Open Res. Software* **2016**, *4* (1), e3.
- (39) Berry, J. D.; Neeson, M. J.; Dagastine, R. R.; Chan, D. Y.; Tabor, R. F. Measurement of surface and interfacial tension using pendant drop tensiometry. *J. Colloid Interface Sci.* **2015**, *454*, 226–237.
- (40) Stalder, A.; Kulik, G.; Sage, D.; Barbieri, L.; Hoffmann, P. A snake-based approach to accurate determination of both contact points and contact angles. *Colloids Surf., A* **2006**, *286* (1–3), 92–103.
- (41) Law, K.-Y.; Zhao, H. *Surface Wetting*; Springer International Publishing Switzerland: 2016.
- (42) Valvatne, P. H.; Blunt, M. J. Predictive pore-scale modeling of two-phase flow in mixed wet media. *Water Resour. Res.* **2004**, *40* (7), W07406.
- (43) Dong, H. *Micro-CT Imaging and Pore Network Extraction*. Ph.D. Dissertation, Department of Earth Science and Engineering, Imperial College London, 2008.
- (44) Dong, H.; Blunt, M. J. Pore-network extraction from micro-computerized-tomography images. *Phys. Rev. E* **2009**, *80* (3), 036307.
- (45) Kim, S.; Santamarina, J. C. Engineered CO₂ injection: The use of surfactants for enhanced sweep efficiency. *Int. J. Greenhouse Gas Control* **2014**, *20*, 324–332.
- (46) Warth, A. D. Relationship between the heat resistance of spores and the optimum and maximum growth temperatures of *Bacillus* species. *J. Bacteriol.* **1978**, *134* (3), 699–705.
- (47) Davis, D.; Lynch, H.; Varley, J. The production of surfactin in batch culture by *Bacillus subtilis* ATCC 21332 is strongly influenced by the conditions of nitrogen metabolism. *Enzyme Microb. Technol.* **1999**, *25* (3–5), 322–329.
- (48) Shapiro, S.; Vining, L. C. Suppression of nitrate utilization by ammonium and its relationship to chloramphenicol production in *Streptomyces venezuelae*. *Can. J. Microbiol.* **1984**, *30* (6), 798–804.
- (49) Onaizi, S. A.; Nasser, M.; Twaiq, F. Adsorption and thermodynamics of biosurfactant, surfactin, monolayers at the air-buffered liquid interface. *Colloid Polym. Sci.* **2014**, *292* (7), 1649–1656.
- (50) Adamson, A. W.; Gast, A. P. *Physical Chemistry of Surfaces*; Interscience Publishers: 1967.
- (51) Jang, S. S.; Goddard, W. A. Structures and properties of newton black films characterized using molecular dynamics simulations. *J. Phys. Chem. B* **2006**, *110* (15), 7992–8001.
- (52) Wang, J.; Ma, T.; Zhao, L.; Lv, J.; Li, G.; Zhang, H.; Zhao, B.; Liang, F.; Liu, R. Monitoring exogenous and indigenous bacteria by PCR-DGGE technology during the process of microbial enhanced oil recovery. *J. Ind. Microbiol. Biotechnol.* **2008**, *35* (6), 619–628.
- (53) Zhang, F.; She, Y.-H.; Li, H.-M.; Zhang, X.-T.; Shu, F.-C.; Wang, Z.-L.; Yu, L.-J.; Hou, D.-J. Impact of an indigenous microbial enhanced oil recovery field trial on microbial community structure in a high pour-point oil reservoir. *Appl. Microbiol. Biotechnol.* **2012**, *95* (3), 811–821.
- (54) Haghghat, S.; Sepahi, A. A.; Mazaheri Assadi, M.; Pasdar, H. Ability of indigenous *Bacillus licheniformis* and *Bacillus subtilis* in microbial enhanced oil recovery. *Int. J. Environ. Sci. Technol.* **2008**, *5* (3), 385–390.
- (55) Bao, M.; Kong, X.; Jiang, G.; Wang, X.; Li, X. Laboratory study on activating indigenous microorganisms to enhance oil recovery in Shengli Oilfield. *J. Pet. Sci. Eng.* **2009**, *66* (1–2), 42–46.
- (56) Shahebrahimi, T.; Fazlali, A.; Motamedi, H.; Kord, S. Experimental and Modeling Study on Precipitated Asphaltene Biodegradation Process Using Isolated Indigenous Bacteria. *Ind. Eng. Chem. Res.* **2018**, *57* (50), 17064–17075.
- (57) Kim, Y.-M.; Park, T.; Kwon, T.-H. Engineered bioclogging in coarse sands by using fermentation-based bacterial biopolymer formation. *Geomech. Eng.* **2019**, *17* (5), 485–496.
- (58) Ghojavand, H.; Vahabzadeh, F.; Shahraki, A. K. Enhanced oil recovery from low permeability dolomite cores using biosurfactant produced by a *Bacillus mojavensis* (PTCC 1696) isolated from Masjed-I Soleyman field. *J. Pet. Sci. Eng.* **2012**, *81*, 24–30.
- (59) Vaz, D. A.; Gudiña, E. J.; Alameda, E. J.; Teixeira, J. A.; Rodrigues, L. R. Performance of a biosurfactant produced by a *Bacillus subtilis* strain isolated from crude oil samples as compared to commercial chemical surfactants. *Colloids Surf., B* **2012**, *89*, 167–174.
- (60) Youssef, N.; Simpson, D.; Duncan, K.; McInerney, M.; Folmsbee, M.; Fincher, T.; Knapp, R. In situ biosurfactant production by *Bacillus* strains injected into a limestone petroleum reservoir. *Appl. Environ. Microb.* **2007**, *73* (4), 1239–1247.
- (61) Varjani, S. J.; Upasani, V. N. Core flood study for enhanced oil recovery through ex-situ bioaugmentation with thermo-and halotolerant rhamnolipid produced by *Pseudomonas aeruginosa* NCIM 5514. *Bioresour. Technol.* **2016**, *220*, 175–182.
- (62) Morikawa, M. Beneficial biofilm formation by industrial bacteria *Bacillus subtilis* and related species. *J. Biosci. Bioeng.* **2006**, *101* (1), 1–8.
- (63) Montagnoli, R. N.; Lopes, P. R. M.; Bidoia, E. D. Assessing *Bacillus subtilis* biosurfactant effects on the biodegradation of petroleum products. *Environ. Monit. Assess.* **2015**, *187* (1), 4116.